

PRELIMINARY ROCK MAGNETIC PROPERTIES OF QUATERNARY BASALTS FROM THE PERȘANI MOUNTAINS (ROMANIA)*

A. ȚUGUI, C. NECULA, C. PANAIOTU

University of Bucharest, Faculty of Physics, E-mail: cristian.panaiotu@g.unibuc.ro

(Received July 2, 2008)

Abstract. Thermomagnetic curves, low field magnetic susceptibility variation, hysteresis parameters, FORC (first order reversal curves) diagrams were measured for representative samples from the main eruption phases in Perșani Mountains. We found that magnetic mineralogy is dominated by the titanomagnetite series with grain size compatible with SD-MD mixture.

Key words: rockmagnetism, paleomagnetism, Quaternary volcanism.

1. INTRODUCTION

Alkali basaltic volcanism in Perșani Mountains represents an important Quaternary alkali basaltic province inside the Carpathians and south-eastern Europe. Recent K-Ar ages combined with paleomagnetic data have demonstrated that the basaltic volcanism in the Perșani Mountains occurred in two relatively short phases [1]. The first one lasted several tens thousands of years around 1.2 Ma and it seems that the inception of the volcanic activity took place in two isolated places and reached the maximum extension during Cobb Mountain Normal Polarity Subchron when larger areas were covered. The second phase started just before 600 ka and was restricted to the central area of the volcanic field. One lava flow of this phase recorded a short-lived reversed polarity event inside Brunhes Normal Chron. Since both Cobb Mountain Normal Polarity Subchron and excursions during the Brunhes Normal Chron are recorded in only few places on the Earth, a new study was started in 2007 to obtain more detailed data about the geomagnetic field behavior during these events combined with a more precise Ar-Ar dating. As a first step in this study we present in this paper new rockmagnetic results obtained from the Perșani Mountains basalts.

* Paper presented at the Annual Scientific Conference, June 6, 2008, Faculty of Physics, Bucharest University, Romania.

2. SAMPLING AND METHODS

For this study we have selected representative samples from the main eruption phases. Samples 2522 (Turzunului Valley) and 2546 (Comana Quarry) have reversed polarity and represent the beginning of the first eruption phase in the Perșani Mts. Samples 2534 and PN6-3 with intermediate directions (Racoș Quarry) and 2548 (Bogata valley) with normal polarity correspond to the main eruption period during the phase 1 which took place inside Cobb Mountain Normal Polarity Subchron. The last two samples, 2555 (Pietrele Valley) and BR3 (Old Bârc Quarry) have both normal polarities and correspond to the last eruption phase during the Brunhes Normal Chron. The location of the samples is presented in [1].

Low-field variation of magnetic susceptibility was investigated using the MFK1-FA Kappabridge (AGICO Inc., 2006). The measurements were executed in 20 distinct fields ranging from 2 to 700 A/m (in one frequency of 975 Hz). The AC magnetic susceptibility was measured as a function of temperature in the range between 20⁰C and 700⁰C using the same Kappabridge with CS3 furnace operating at a low field of 200 A/m and a frequency of 975 Hz. The heating rate was 10⁰ /min. To avoid mineral reactions with atmospheric oxygen, the measurements were performed in a flowing argon atmosphere.

Hysteresis loops were measured at room temperature using Princeton Measurements Corporation VSM (vibrating sample magnetometer) 3900 (2007), with a maximum saturating field of 1T. The parameters M_s , M_{rs} and H_c (saturation magnetization, remanent magnetization and coercive force respectively) were determined after correction for the para- or diamagnetic contribution to the total magnetic moment. In order to obtain H_{cr} (coercivity of remanence) samples were then demagnetized in an alternate field and given an SIRM (saturation isothermal remanent magnetization) which was demagnetized in a stepwise backfield up to a maximum of -1T.

FORC measurements were conducted using the same PMC VSM 3900 magnetometer. To construct a FORC diagram, 111 first-order reversal curves were measured using a saturating field of 1T. The FORC data processing was performed using FORCinel software developed by [2]. The calculation of first-order reversal curve (FORC) diagrams use locally weighted regression smoothing and can perform an optimum smoothing factor calculation.

All measurements were performed at the Paleomagnetic Laboratory, University of Bucharest.

3. RESULTS AND DISCUSSIONS

The Curie temperature defines the transition from ferrimagnetic to paramagnetic ordering, giving thus information about magnetic mineralogy. Based on changes in magnetic susceptibility during heating, three different groups of

magneto-mineralogical behavior can be distinguished within the Perșani Mountains (Fig. 1). First group (samples 2534 and 2546) display Curie temperatures between 100° and 200°C, indicating the presence of a high amount of titanomagnetite. The second group, comprising samples 2522 and PN63, shows a slight monotonic increase of magnetic susceptibility, with the increasing temperature, until reaches the Curie temperature at 580°C indicating magnetite as the final product. The third group (samples 2555, 2548 and BR3) presents two phases: one, rich in titanomagnetite, with Curie temperature between 100 and 200°C, and the other, poor in titanomagnetite, with Curie temperature between 500 and 600°C.

An improved calibration curve for the compositional dependence of the Curie temperature of titanomagnetite on the basis of temperature-dependent magnetic susceptibility curves measured on synthetic titanomagnetites in the Fe-Ti-O system were developed by [3]. According to this study, Curie temperatures between 100 and 200°C corresponds to an ulvospinel content, X_{Usp} , between 0.4 and 0.6, the first group and the first phase of the third group having thus an intermediate chemical composition of titanomagnetite in the magnetite (Fe_2O_3)-ulvospinel ($FeTiO_4$) solid solution series. For the second phase of the third group, Curie temperature between 500 and 600°C indicates ulvospinel content, X_{Usp} , between 0.0 and 0.2, this phase being thus poor in titan.

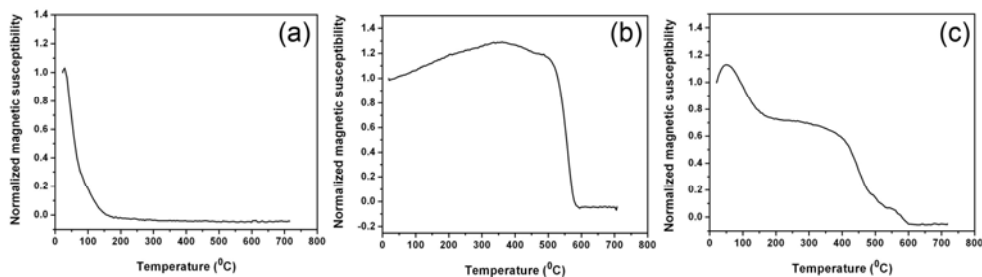


Fig. 1 – Temperature dependence of magnetic susceptibility for representative samples from Perșani Mountains (magnetic susceptibilities normalized to the room temperature values): a) first group; b) second group; c) third group (see text).

Low-field variation of magnetic susceptibility can yield a quick and routine indication of the main magnetic mineral in the rock under study. Two groups can be observed in our samples based on variation of magnetic susceptibility versus field. First group (samples PN63 and 2522) show no variation or very weak one of magnetic susceptibility with increasing field, this behavior being associated to pure magnetite, [4]. For the second group the susceptibility increases with field intensity rapidly, which is a characteristic feature of titanomagnetite (e.g., [4, 5, 6, 7, 8]). The second group can be further subdivided in two subgroups regarding the shape of variation curves. First subgroup (samples BR3, 2548, 2555) displays a variation more or less linearly in the entirely field range obeying thus to the Rayleigh law for

multidomain particles, [5]. This subgroup corresponds with the third group highlighted by Curie temperatures, characterized by a bimodal distribution of titanomagnetite (high and low content of titanium phases). In the second subgroup (samples 2534, 2546) the susceptibility increases with field relatively rapidly, but the increase is not linear in the entire field range, being linear only up the field of 100 A/m. Above this field, the susceptibility increase is slower, the curve being slightly curved and convex in shape. These specimens evidently obey the Rayleigh law only in the fields up to 100 A/m, in the higher fields resembling the cumulative distribution function known from statistics, defined by [9]. The second subgroup corresponds with first group evidenced by Curie temperature characterized by a single phase, rich in titanium. The above two types of curves correspond to the theoretically expected curves.

According to [4], index that characterizes the maximum susceptibility variation with field, $V_m = 100(k_{\max} - k_{\min})/k_{\min}$, where k_{\max} and k_{\min} are the maximum and minimum susceptibilities, respectively, measured during one measuring run, the V_m values being given in %) varies with chemical composition of titanomagnetite which is manifested in variability of the Curie temperatures. In Fig. 2, low values of V_m (from 0 to 10%) of our samples are correlated with almost pure magnetite highlighted by Curie temperatures between 500 and 600°C (samples PN 63 and 2522). Higher values of V_m index (above 30%) indicate the presence of high amount of titanomagnetite pointed out by Curie temperature between 100 and 200°C (samples BR3, 2546, 2548, 2534 and 2555). All data from Perşani Mountains overlap quite well the collection of the specimens published by [4], comprising young alkaline volcanic rocks of the České středohoří Mountains whose magnetic minerals are represented by substituted titanomagnetite.

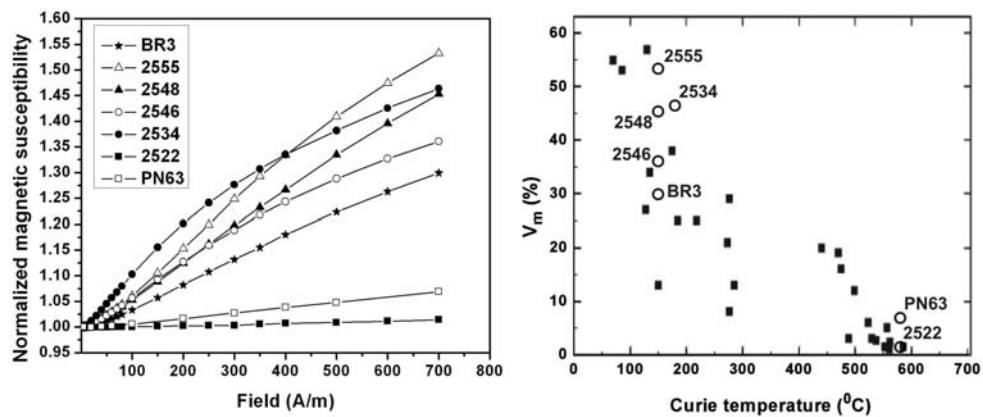


Fig. 2 – a) Susceptibility *versus* field variation curves for representative samples from Perşani Mountains; b) correlation between V_m parameter, [4], and Curie temperatures: open circles – data from Perşani Mountains; black squares – data published by [4], representing titanomagnetite – dominated rocks.

Hysteresis loops provide the most simple and fundamental quantities to estimate domain state of the remanence carriers. All samples reach saturation until 300mT, suggesting that low coercivity minerals (magnetite like) dominate the magnetic mineralogy (Fig. 3). Three types of shapes of hysteresis loops are evidenced. First type belonging to sample 2522 is very thin and displays certain linearity. A bulk coercive force of 3.7 mT suggests that this sample is rich in MD particles. Second type, characterizing five samples (2534, 2546, 2548, 2555, BR3), is “wasp-waisted”, indicating mixed SP-SD populations [10]. Bulk coercive force has intermediate values between 3.7 and 27mT reflecting also a mix of SD-MD particles. Third type, belonging to sample PN63, is very large having more pronounced S shape. The bulk coercive force is almost one order of magnitude larger than for 2522 sample ($H_c = 26\text{mT}$), reflecting thus higher amount of elongated SD particles [11].

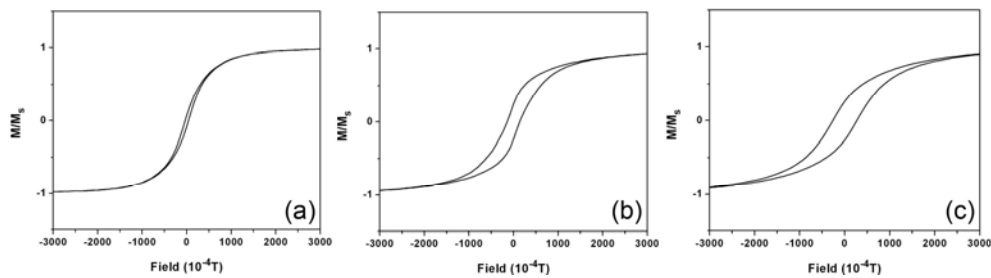


Fig. 3 – Hysteresis loops for representative samples from Perșani Mountains: a) first type, b) second type, c) third type (see text). All curves are corrected for para- and diamagnetic contributions.

The standard procedure to estimate domain state in rock magnetism is the Day plot (M_{rs}/M_s versus H_{cr}/H_c , [12]). All our data plots in the PSD region (Fig. 4), following the general hyperbolic trend of the model SD + MD mixing curves for magnetite calculated by [13], except BR3, falling somewhat above mixing curve 3, just between the theoretical mixing curves for TM60 (titanomagnetite with $X_{Usp} = 0.6$). According to these curves magnetic grain size varies from coarse, toward MD region (sample 2522) to medium and fine, toward SD region (sample PN63). The same mixing model for TM60 predicts curves that do not fit the data at all. Alongside BR3, also samples 2555 and 2522 are situated between the TM60 mixing curves but they do not follow the characteristic abrupt trend of SD→MD transition curves. Being known that $\text{Fe}_{2.8}\text{Ti}_{0.2}\text{O}_4$ (i.e., $X_{Usp} = 0.2$) behaves more or less like Fe_3O_4 ($X_{Usp} = 0.0$), [13], one explanation is that the samples belonging to the third group evidenced by Curie temperature have a greater concentration of titanomagnetite with X_{Usp} between 0.0 and 0.2, dominating thus the magnetic properties of the samples. For sample BR3 the reverse is probably happening, a greater fraction of titanomagnetite with X_{Usp} between 0.4 and 0.6 leading to a more like TM60 behavior. We don't have yet an explanation for samples 2534 and 2546, being necessary further investigations to make understandable this behavior.

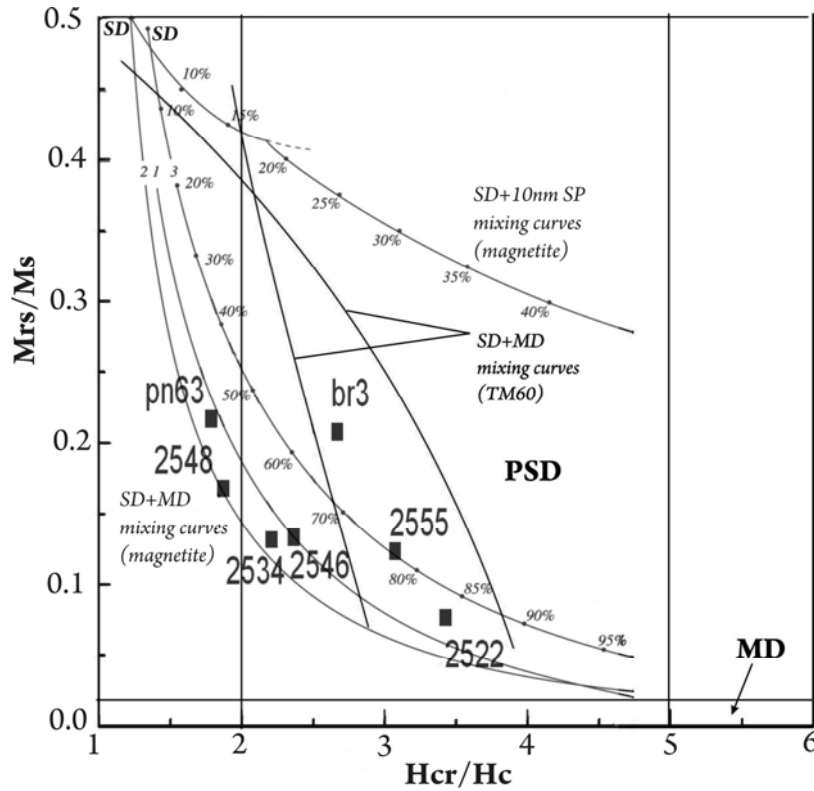


Fig. 4 – Hysteresis data from Perşani Mountains compared with theoretical mixing curves developed by [13].

Recently, a new technique for studying hysteresis properties has been introduced, based on the measurement of first-order reversal curves (FORC). The FORC technique has been claimed to provide more detailed characterization of hysteresis properties, than can be obtained from the bulk hysteresis parameters, [14] and [15].

The measurement of a first-order reversal curve (FORC) diagram starts with saturating a sample in a large positive magnetic field. Then, the field is decreased to a reversal field H_a and a partial hysteresis curve (a first-order reversal curve) is measured as the applied field (H_b) increases from H_a back to saturation. This measurement procedure is repeated for a number of values of H_a to obtain a set of FORCs. The magnetization at the applied field H_b on the FORC with reversal point H_a is denoted by $M(H_a, H_b)$, where $H_b \geq H_a$. The FORC distribution is defined as the mixed second derivative $\rho(H_a, H_b) = -\partial^2 M(H_a, H_b) / \partial H_a \partial H_b$ [14] and [15]. For plotting, the FORC distribution coordinates (H_a, H_b) are conventionally rotated by 45° to $H_c = (H_b - H_a)/2$, $H_u = (H_b + H_a)/2$. A FORC diagram is a contour plot of a FORC distribution with H_u and H_c on the vertical and horizontal axes, respectively

[15]. In order to calculate the FORC distribution at any point P, a least squares fit to $M(H_a, H_b)$ is performed over a square grid of points surrounding P. The interpretation of a FORC diagram is relatively straightforward for samples containing single-domain (SD) magnetic grains. The H_c coordinate of the FORC distribution peak represents the mean switching field of a SD ensemble. For noninteracting SD grains, the FORC distribution is narrow in vertical direction and elongated along the H_c axis (the elongation reflects the grain size-shape distribution in a sample). Regarding the effect of magnetostatic interactions on FORC distributions, it is generally accepted that a local interaction field, if present, manifests itself in an increased vertical spread of a FORC distribution, symmetric with respect to the H_c axis [14]. The effect of a mean interaction field may include stretching, shifting, and breaking the symmetry of a FORC distribution (e.g., [14, 16, 17, 18]). A FORC diagram may simultaneously manifest the signatures from both local and mean interaction fields.

Sample PN63 looks like an SD particle with closed concentric contours about a central peak at $H_c = 25\text{mT}$ (Fig. 5). The spreading along the H_u axis and the symmetry around the $H_u = 0$ proved that this sample is affected by a local interaction field. Sample 2522 has a much larger spread of the outer contours, less closed inner contours, and a smaller tail toward high coercivities. Its contours remain extended along the H_c axis, giving the PSD FORC distribution a characteristic three-lobe configuration with lobes extending in the $+H_u$ and $-H_u$ directions and along the H_c axis, [19]. Sample 2555 have even less closed contours than sample 2522 but the three lobes are still visible, reflecting thus the PSD states of magnetic grain size. Sample BR3 is similar with sample 2555 but with an extended tail toward high coercivities. Samples 2534 and 2548 have a similar FORC configuration, with closed contours around a central peak ($H_c \sim 5\text{mT}$) with almost no spreading (the three-lobes configuration is missing) along the H_u axis which indicates a noninteracting ensemble of particles. Sample 2546 shows a bimodal FORC distribution with two peaks, one smaller, with closed contour centered at $H_c \sim 20\text{mT}$ and the most intense with unclosed contours, reflecting mixed SD-MD populations. As the same time the first peak centered at $H_c \sim 20\text{mT}$ is situated below the $H_u = 0$ while the second peak lies above the $H_u = 0$, this asymmetry being referable to the effect of a mean interaction field.

Another remarkable feature which can be observed in FORC distribution is that in all samples containing titanomagnetite the interacting field is dramatically reduced.

4. CONCLUSIONS

The rockmagnetic results show that the magnetic mineralogy is dominated by the titanomagnetite series. The samples can be divided in 3 categories according to the magnetic mineralogy: a) magnetite only; b) high Ti ($X_{\text{Usp}} = 0.4\text{--}0.6$) content; c) a mixture of the previous two categories.

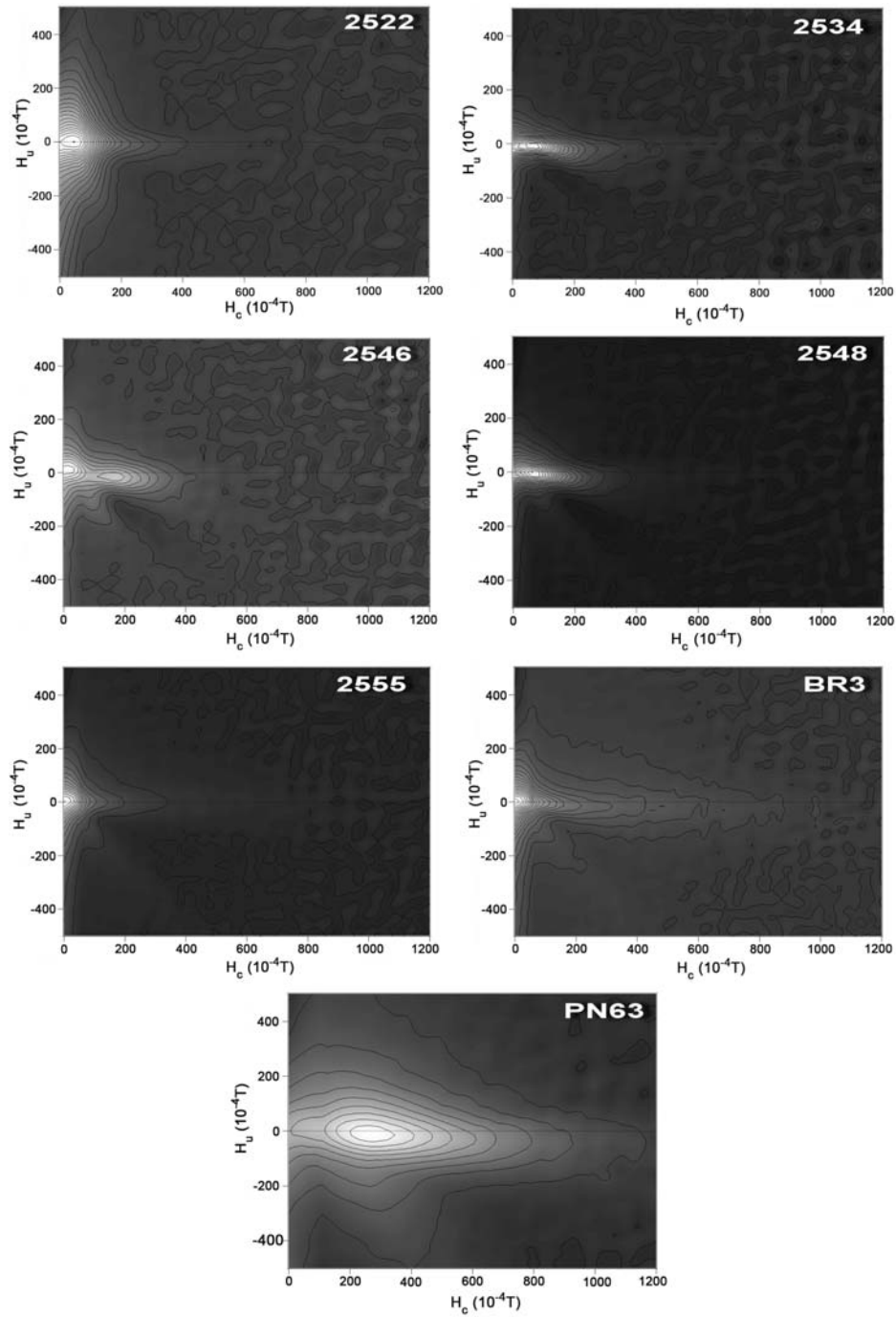


Fig. 5 – FORC diagrams for the representative samples from Perşani Mountains.

Hysteresis properties and FORC diagrams have shown that the magnetic granulometry is compatible with SD-MD mixture. FORC distributions also reveal diminished interaction fields in the presence of Ti. There is no systematic trend in the rockmagnetic data which can be associated with a particular time of eruption. Petrographic and mineralogic studies are in progress to establish if the magnetic properties of the studied basalts reflect the cooling rate of lava flows or some heterogeneity of the initial magmas.

Acknowledgements. We thank to the authors of the FORCinel for the permission to use there software. This work was supported by CNCSIS ID-974 grant 400/2007.

REFERENCES

1. C.G. Panaiotu, Z. Pecskay, U. Hambach, I. Seghedi, C.E. Panaiotu, I. Tetsumaru, M. Orleanu, A. Szakacs, *Short-lived Quaternary volcanism in the Persani Mountains (Romania) revealed by combined K-Ar and paleomagnetic data*, *Geologica Carpathica*, **55**, 333–339 (2004).
2. R. J. Harrison, and J. M. Feinberg, *FORCinel: An improved algorithm for calculating first-order reversal curve distributions using locally weighted regression smoothing*, *Geochemistry, Geophysics, Geosystems*, **9**, Q05016 (2008), doi:10.1029/2008GC001987.
3. D. Lattard, R. Engelmann, A. Kontny, and U. Sauerzapf, *Curie temperatures of synthetic titanomagnetites in the Fe-Ti-O system: Effects of composition, crystal chemistry, and thermomagnetic methods*, *J. Geophys. Res.*, **111**, B12S28 (2006), doi:10.1029/2006JB004591.
4. František Hrouda, Marta Chlupáčová, Štěpánka Mrázová, *Low-field variation of magnetic susceptibility as a tool for magnetic mineralogy of rocks*, *Physics of the Earth and Planetary Interiors*, **154**, 323–336 (2006).
5. M. Jackson, B. Moskowitz, J. Rosenbaum, C. Kissel, *Field dependence of AC susceptibility in titanomagnetites*, *Earth Planet. Sci. Lett.*, **157**, 129–139 (1998).
6. H. De Wall, *The field dependence of AC susceptibility in titanomagnetites: implications for the anisotropy of magnetic susceptibility*, *Geophys. Res. Lett.*, **27**, 2409–2411 (2000).
7. Hrouda F., *Low-field variation of magnetic susceptibility and its effect on the anisotropy of magnetic susceptibility of rocks*, *Geophys. J. Int.*, **150**, 715–723 (2002).
8. DE Wall H., and L. Nano, *The use of field dependence of magnetic susceptibility for monitoring variations in titanomagnetite composition – a case study of basanites of Vogelsberg 1996 Drillhole, Germany*. *Stud. Geophys. Geod.*, **48**, 767–776 (2004).
9. P.M. Kruiver, M.J. Dekkers, D. Heslop, *Quantification of magnetic coercivity components by the analysis of acquisition curves of isothermal remanent magnetization*, *Earth Planet. Sci. Lett.*, **189**, 269–276 (2001).
10. Karl Fabian, *Some additional parameters to estimate domain state from isothermal magnetization measurements*, *Earth and Planetary Science Letters*, **213** 337–345 (2003).
11. D.J. Dunlop, O. Ozdemir, *Rock magnetism: fundamentals and frontiers*, Cambridge University Press, UK, 1997.
12. R. Day, M. Fuller, and V. A. Schmidt, *Hysteresis properties of titanomagnetites: Grain size and composition dependence*, *Phys. Earth Planet. Inter.*, **13**, 260–267 (1977).
13. D. J. Dunlop, *Theory and application of the Day plot (M_{rs}/M_s versus H_{cr}/H_c): 1. Theoretical curves and tests using titanomagnetite data*, *J. Geophys. Res.*, **107**, B3, 2056 (2002), doi:10.1029/2001JB000486.
14. C. R. Pike, P. A. Roberts, and K. L. Verosub, *Characterizing interactions in fine magnetic particle systems using first order reversal curves*, *J. Appl. Phys.*, **85**, 6660–6667 (1999).

15. A. P. Roberts, C. R. Pike, and K. L. Verosub, *First order reversal curve diagrams: A new tool for characterizing the magnetic properties of natural samples*, J. Geophys. Res., **105**, 28, 461–28, 475 (2000).
16. C. R. Pike, C. A. Ross, R. T. Scalettar, and Zimanyi G., *First-order reversal curve diagram analysis of a perpendicular nickel nanopillar array*, Phys. Rev. B, **71** (2005), doi:10.1103/PhysRevB.71.134407.
17. A. Stancu, C. Pike, L. Stoleriu, P. Postolache, and D. Cimpoesu, *Micromagnetic and preisach analysis of the first order reversal curves (FORC) diagram*, J. Appl. Phys., **93**, 6620–6622 (2003).
18. M. Winklhofer, and G. T. Zimanyi, *Extracting the intrinsic switching field distribution in perpendicular media: A comparative approach*, J. Appl. Phys., **99**, 08E710 (2006), doi:10.1063/1.2176598.
19. A. V. Smirnov, *Low-temperature magnetic properties of magnetite using first-order reversal curve analysis: Implications for the pseudo-single-domain state*, Geochem. Geophys. Geosyst., **7**, Q11011 (2006), doi:10.1029/2006GC001397.